TECHNICAL ARTICLE

PreDICT: a graphical user interface to the DICVOL14 indexing software program for powder diffraction data

Justin R. Blanton,[1] Robert J. Papoular [2,a)] and Daniel Louër[3]

[1]*International Centre for Diffraction Data, Newtown Square, PA 19073-3273*
[2]*Saclay Institute for Matter and Radiation (IRAMIS), Leon Brillouin Laboratory, CEA/CEN-Saclay, 91191 Gif-sur-Yvette, France*
[3]*Retired from Centre National de la Recherche Scientifique and Université de Rennes I, Rennes, France*

A straightforward intuitive user-friendly compact graphical interface, PreDICT (Premier DICVOL Tool) has been developed to take full advantage of the new capabilities of the most recent version of the DICVOL14 Indexing Software. The latter, an updated version of DICVOL04, includes optimizations, e.g. for monoclinic and triclinic cases, a detailed review of the input data from the indexing solutions, cell centering tests, as well as the handling of a moderate number of impurity peaks. Among the most salient features of PreDICT, one can mention the ability (1) to use 2θ non-equistepped input 1D X-ray powder diffraction patterns as can be obtained from 2D detectors, (2) to strip laboratory data from its $K\alpha_2$ contribution when present, (3) to generate 2θ equistepped output 1D X-ray powder diffraction patterns in both the ".XY" and ".GSA" formats. In addition, PreDICT allows for the following features: (1) full access to the native DICVOL14 input/output ASCII file system is retained, (2) for any selection of a DICVOL14 suggested unit cell, all predicted Bragg peaks up to a certain $2\theta_{MAX}$ value are clearly displayed and indicated, thereby emphasizing the contribution of the unaccounted peaks (if any) to the 1D X-ray powder diffraction pattern under current investigation. © *2019 International Centre for Diffraction Data.* [doi:10.1017/S0885715619000514]

Key words: graphical interface, indexing, DICVOL14, powder diffraction

I. INTRODUCTION

The ubiquitous freely available DICVOL indexing software is now about 50 years old. Developed in an academic context over several years (Louër and Louër, 1972; Boultif and Louër, 1991, 2004; Louër and Boultif, 2014), some of its previous versions (up to DICVOL06) can be found incorporated in several software packages involving a graphical user interface (GUI). Among them: FOX (Favre-Nicolin and Černý, 2002), EXPO (Altomare *et al.*, 2013), WinPLOTR (Roisnel and Rodriguez-Carvajal, 2001), DASH (David *et al.*, 2006), and MATCH! (Putz and Brandenburg, 2018). With the field of indexing diffraction powder data still exploring new approaches today (Coelho, 2017), we decided to develop our own GUI as a free service to the X-ray and Neutron Powder Diffraction community. Strictly dedicated to running DICVOL14 and entirely compliant with the file system of the latter, it is compact, intuitive, easy-to-use, and user-friendly.

Attempts at successful indexing of powder diffraction patterns without conscience are doomed to failure. The reader is referred to a classic review (Langford and Louër, 1996) for general considerations about the essentials of powder diffraction, to NBS/NIST Conference papers (Shirley, 1980; Louër, 1992) for a discussion about the required quality of the X-ray diffraction data, and lastly to the paper discussing DICVOL14 (Louër and Boultif, 2014) new features, as well as to the latest version (v2.17) of the DICVOL14 user manual and software.

We conclude this paper by briefly discussing three examples, with a single goal in sight, namely to emphasize PreDICT various functionalities, rather than to advocate the quality of the X-ray diffraction data to be successfully used with PreDICT/DICVOL14. We refer the reader to previously published work regarding various aspects of DICVOL14 handling of triclinic cases, including difficult ones involving a longer axis or a dominant zone (Louër and Boultif, 2014, Section B and Table I, p. S10).

II. PreDICT FEATURES

The software is written in Java (required version: Java Runtime Environment [JRE] 8 or higher). It runs on Windows PC's (XP or later).

Amongst PreDICT most salient characteristics:

1. *Input file formats* (ASCII only): Powder ".CIF", ".XY", ".XYE", ".UXD", and ".GSA". For all the other ASCII or binary input formats, please first use the freely available PowDLL software (Kourkoumelis, 2013) for preliminary conversion to one of the above.
2. *Wavelength*(s) [in Å]: Monochromatic or ($K\alpha_1$, $K\alpha_2$) pair.
3. *Background automatic retrieval*, using an algorithm published by Sonnefeld and Visser (1975).
4. *Smoothing*, using a Savitzky–Golay filter (Savitzky and Golay, 1964).
5. *$K\alpha_2$ stripping*, using the widespread Rachinger method (Rachinger, 1948).

---

a)Author to whom correspondence should be addressed. Electronic mail: robert.papoular@cea.fr

6. *Automatic peak selection*. Once this step has been carried out, the user retains the flexibility to manually dispose of dubious or select additional peaks. PreDICT automatically keeps track of the latest peak selection for a given histogram and restores the peak file when the same diffractogram is used again. The latter information is saved in ".XML" format in the following directory and file: *C:\Users\xxxx \AppData\Roaming\ICDD\PreDICT\preferences.xml*, where xxxx features the User's name, pseudo or alias. The 3-4-5-6 data processing selections can be saved as well in this *preferences.xml* file and restored at any time.

7. *Output file formats* (ASCII only): Equistepped interpolated ".XY" and ".GSA" for both the raw and processed 1D data-files. The ".GSA" format, which requires equistepped data, is included to facilitate subsequent Le Bail (Le Bail, 2005) and Rietveld (Rietveld, 1969) refinements using the freely available GSAS software (Larson and Von Dreele, 2004).

8. *Graphics Hardcopy* output at any stage during the data processing, in both the ".PNG" and ".JPG" formats.

III. OPTIMAL USE OF THE SOFTWARE

The indexing of powder diffraction patterns is a demanding application of the powder diffraction method. The first and mandatory requirement is to not compromise with the quality of the input raw 1D powder diffraction data. Synchrotron and/or laboratory monochromatic X-ray sources should be used whenever available. The 2θ-stepsize should ideally not be larger than $0.01°/0.02°$ according to the FWHM of the diffraction lines and the wavelength used. High-quality counting statistics is also required (e.g., for laboratory data collection with scintillation detectors, suitable measurements can be performed overnight over an angular range appropriate for indexing purposes). The remaining recommendations, briefly reported below, are described in detail in the previously mentioned papers discussing the various iterations of the DICVOL software:

(1) The precise positions of the (N_{Total}) Bragg reflections extracted in the low angle region with PreDICT can be input in the program (e.g., 40). Among them, only the first N lines at low 2θ angles (corresponding to the region where the overlap of reflections is minimal) are used for searching unit cells. For most cases involving materials featuring a moderate unit cell volume, $N = 20$ to 25 is generally selected (as shown for instance on Figure 1). Note that in the case of a large or short cell parameter (dominant zone), N often needs to be appreciably >20.

(2) The absolute error $\Delta(2\theta)$ must be selected according to (i) the resolution (FWHM of the diffraction line profile) and (ii) the wavelength used for collecting the powder data. For instance, in the case of laboratory data collected with $CuK\alpha_1$, $|\Delta(2\theta)|$ is usually taken as $0.03°$ (2θ), which is the default value in DICVOL14, except for the triclinic search when it is carried out on its own $[0.025°$ $(2\theta)]$. [See § III. A and III.B.ii in Louër and Boultif (2014).] This error interval is of prime importance in the dichotomy algorithm. Sometimes it must be reduced, for instance in the case of high resolution and precise patterns, large cell volumes, and even for laboratory triclinic diffraction data in some cases (e.g., involving partial geometric ambiguities).

(3) High lattice symmetry solutions should be searched first. As suggested by the DICVOL14 input panel displayed in Figure 2, the following trial sequence is advocated: (i) cubic–tetragonal–hexagonal–orthorhombic, (ii) monoclinic, (iii) triclinic. [Sequences (i) and (ii) can also be joined together.]

(4) Because the search for a triclinic solution is carried out in reciprocal Q-space, as opposed to the other lattice symmetry searches (which are thus carried out in direct R-space), and uses triclinic lattice-dependent estimated cell volume to define a volume range, the search should preferably be carried out independently on its own.

(5) Although ideally powder data for a single phase should preferably be used, a tolerance for spurious lines is accepted in DICVOL14. It is a user's decision to introduce a maximum number "Imp" of accepted spurious lines in the subset of N lines used for searching solutions. This must be pondered carefully, since additional variables are then introduced in the mathematical problem. Two options are proposed, respectively, involving a positive number "Imp" and a negative number "−Imp", both associated with the allowed maximum number of impurities. In the second case ("−Imp"), the number of impurities is sequentially incremented from 0 to Imp and DICVOL14 stops the scanning for that value of the increment for which a solution is found (see example reported in Section V). This latter option is more efficient than the former ("Imp"), albeit more time-consuming.

(6) As noticed in previous papers, a correct cubic unit cell may not feature the highest figures of merit (FOMs): M (N) (de Wolff, 1968) and F(N) (Smith and Snyder, 1979).

(7) At the end of a DICVOL14 run, a pop-up window will open in the PreDICT screen, listing the found unit cells with minimal information (lattice parameters including the corresponding volume of the unit cell and zero 2θ offset) and the classical FOMs, as displayed in Figure 3. This is only one part of the DICVOL14 output. The user is urged to read through the complete original ASCII files generated by DICVOL14 for more information, which are automatically created in the PC working directory that also contains the input 1D powder diffraction data. Firstly, the file PreDICT_OUTPUT.txt sequentially lists each found solution followed by the displayed analysis of the N_{Total} input lines from the cell parameters suggested by the N line subset. It is the user's choice to decide whether to reject a solution involving unindexed lines or to explain the latter. Secondly, the PreDICT_OUTPUT.ORD file gives a detailed evaluation for the five solutions ranked from best to worst achieving the highest de Wolff FOMs. It emphasizes (i) the quality/deficiency of each fitted reflection (in poor indexing cases, a single selected line may be ascribed to more than one Miller index triplet or to none), and (ii) the proposed centering of the found lattices. Both these files should be consulted to check if the suggested unit cells, found from the first N lines, satisfactorily index the N_{Total} input lines.

IV. A TYPICAL EXAMPLE INVOLVING A 1D SIMULATED DATASET

Only high-quality X-ray/neutron diffraction data should be used for indexing. The aim of this first example (described in Figure 4) using simulated data is to warn the reader against high symmetry cases. The various FOMs, M(N), F(N), but also the zero offset and the cell volume should be used with
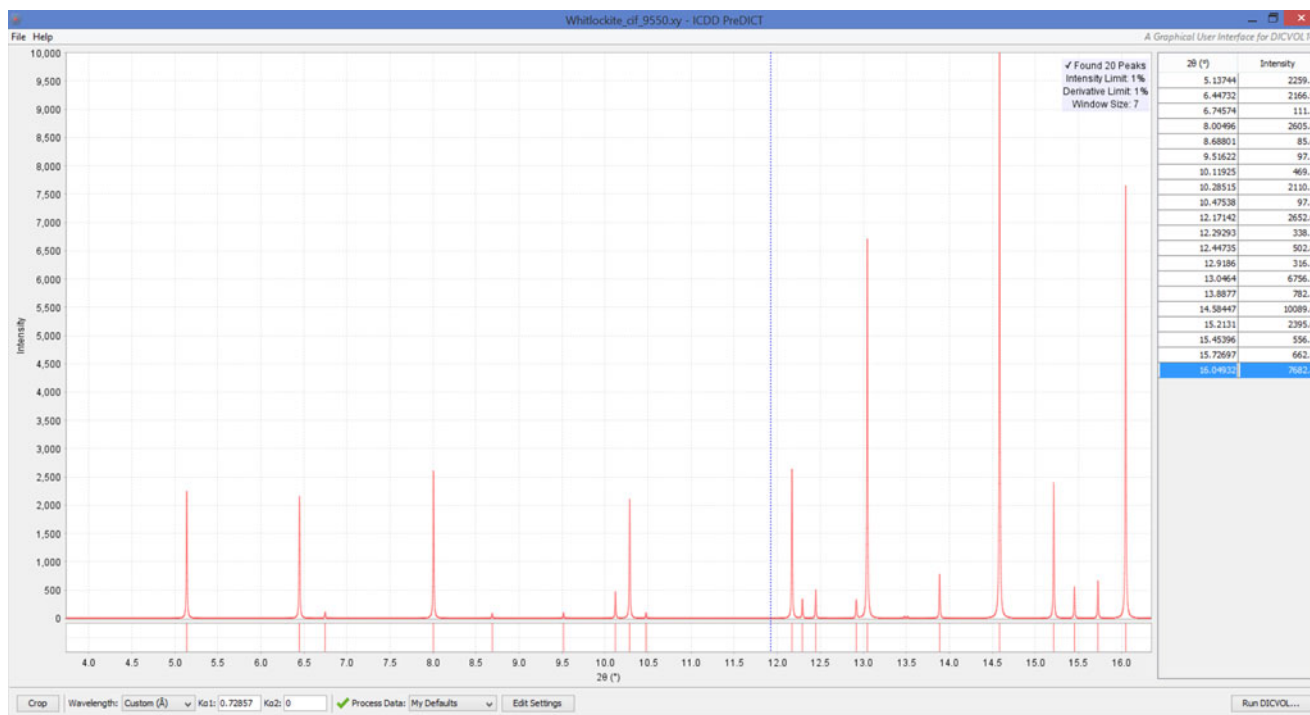
Figure 1.   (Colour online) PreDICT window display after the selection of 20 Bragg peaks to be used for indexing. The simulated monochromatic ($\lambda = 0.72857$ Å) X-ray diffraction powder dataset for Manganese-Whitlockite was calculated from a single-crystal CIF (#9550) obtained from the American Mineralogist Crystal Structure Database accessed through the MINDAT.org website and computed by making use of the free CCDC/MERCURY software.
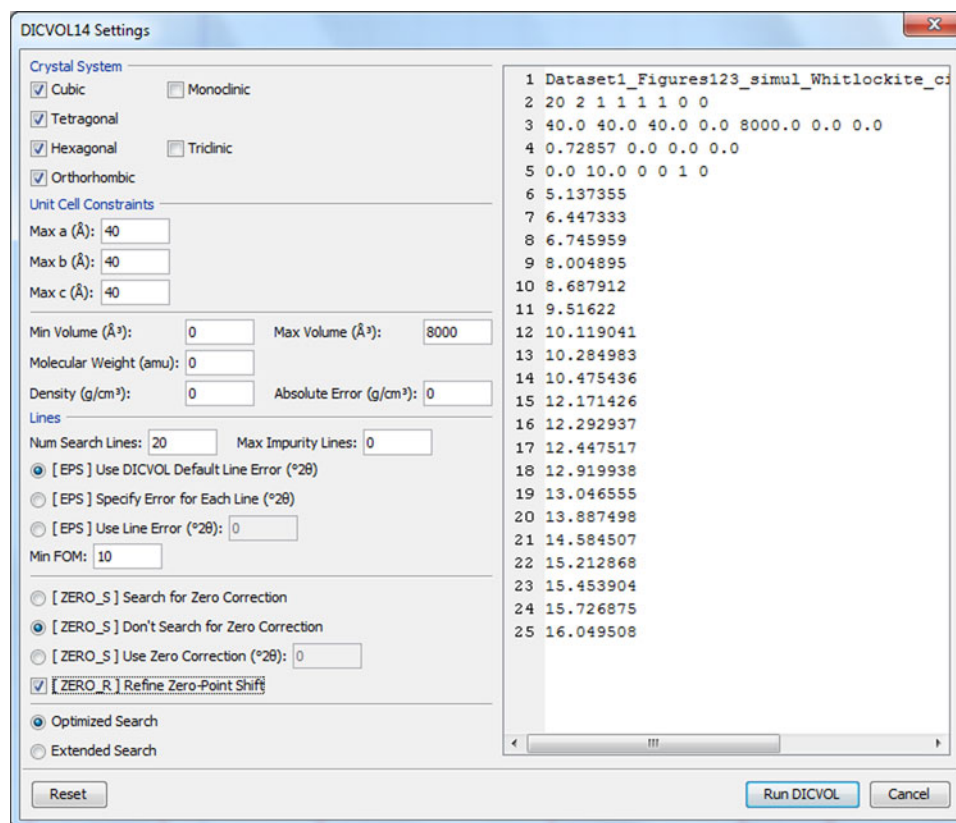

Figure 2.   (Colour online) The dual window panel used to create the pristine DICVOL14 input file. The user feeds in information on the left. The DICVOL14 input file appears on the right and is updated on the fly. In the latter, a default value appear as 0 (if integer) or 0.0 (if real). Note, in particular, the non-default selections: (i) the unit cell constraints (maximum allowed $a = b = c = 40$ Å > 25 Å), (ii) the maximum allowed volume (8000 Å^3), and (iii) the marked (ZERO_R) option. Finally, note the request for an Optimized Search.

Figure 3.   (Colour online) After a successful DICVOL14 run : (i) a list of suggested unit cells is displayed with minimal information. (ii) Once a specific solution is selected (highlighted), all the related calculated Bragg peak positions are graphically displayed (blue marks) below the peaks used for the indexing. In good cases such as the one shown in the figure, Bragg peaks not selected for indexing will now become accounted for (black oval).
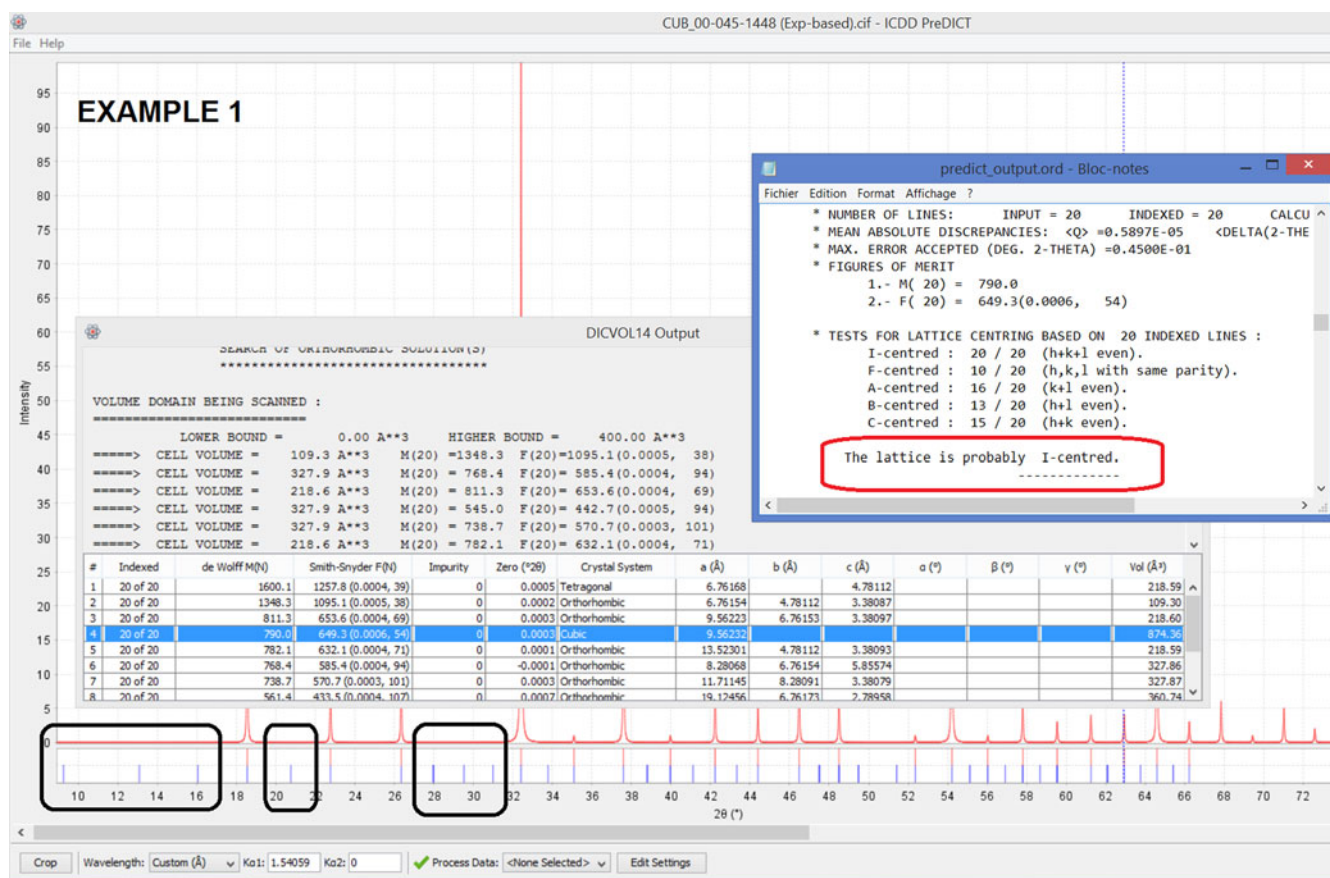

Figure 4.   (Colour online) Example 1: Monochromatic CuKα₁ simulation of cubic Cu_2FeSbO_6. A PreDICT input powder ".CIF" file is first obtained using SIeve+ and the PDF-4+ 2018 database (PDF card 00-045-1448). It is then read into PreDICT, 20 indexing peaks are selected and DICVOL14 runs. Many unit cells are found that include the correct cubic one which only ranks down as #4, FOM-wise. For this latter symmetry, all 20 selected peaks are accounted for, and many calculated indexed peaks are found to have zero intensities [black boxes], strongly suggesting a centering of the unit cell. The pristine DICVOL14 [.ORD] file yields the answer … I-centering … and must thus be compulsorily and thoroughly checked.
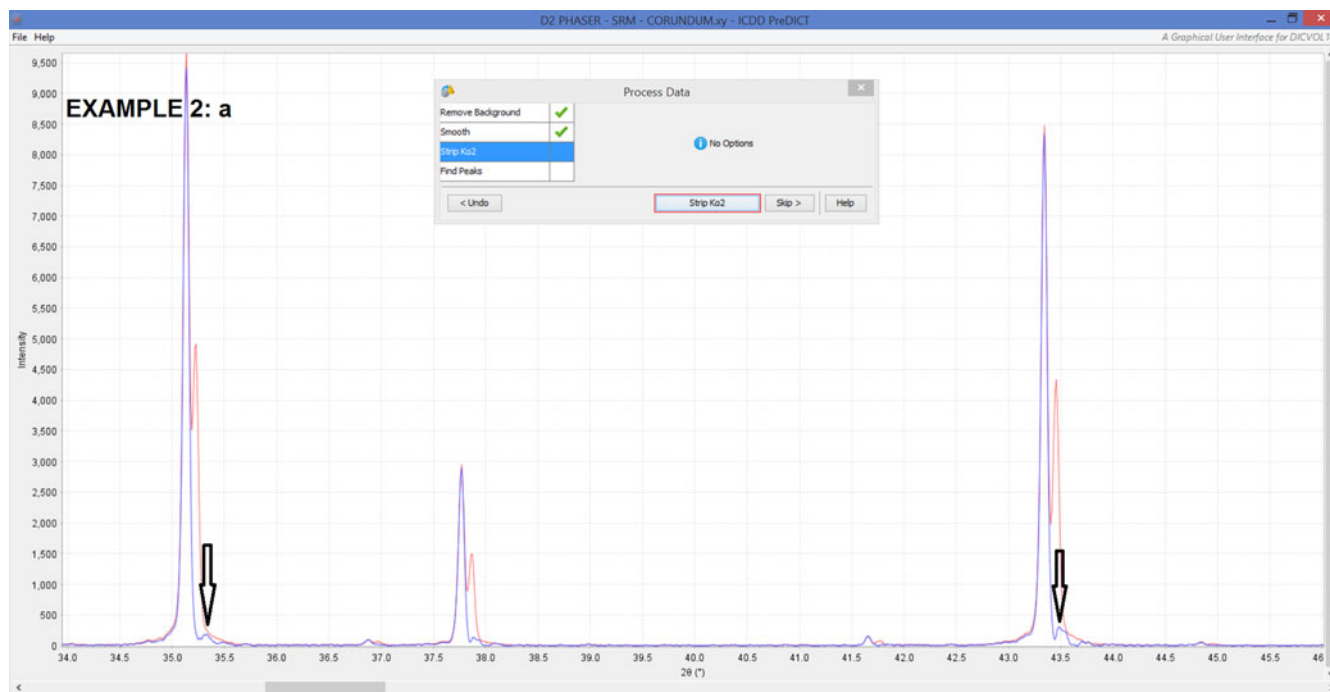
Figure 5. (Colour online) Example 2(a): Polychromatic $CuK\alpha_1 K\alpha_2$ selected region of raw 1D X-ray diffraction data from a D2 PHASER diffractometer. The measured sample is SRM (corundum). The raw data are first smoothed (red line) and subsequently the $CuK\alpha_2$ contribution is removed. Note the remnant peaks because of the imperfect removal of the $CuK\alpha_2$ contribution, which sets limits on trustable weak lines and thus on what can be expected from the indexing process: use synchrotron or laboratory monochromatic radiation whenever available!

care and as indicative of a potential correct indexing only. A higher-symmetry unit cell (e.g., cubic) is always worth checking even if it does not rank first among the solutions found by DICVOL14 and does not feature the highest FOMs! SIeve +/PDF-4+ (Fawcett et al., 2017) offer a most convenient way to obtain simulated diffraction 1D histograms. An alternative is to use the freely available CCDC/MERCURY software (Macrae et al., 2008).
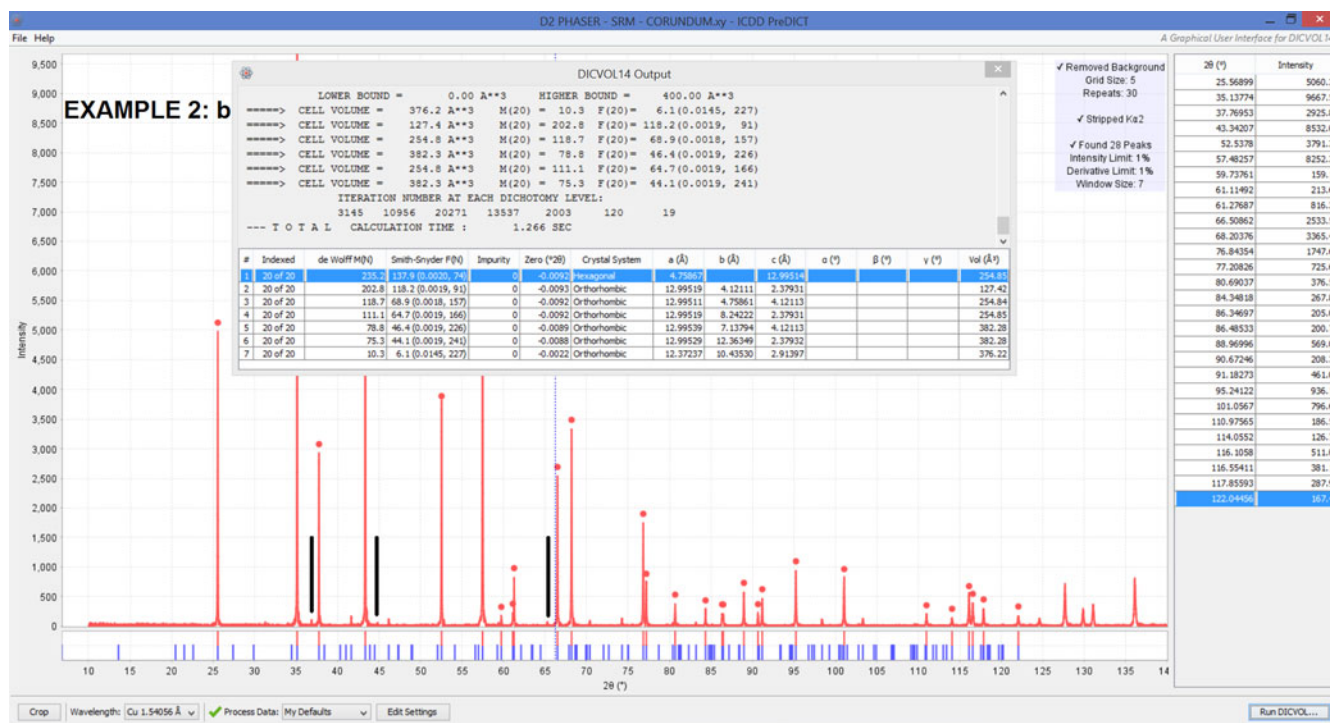

Figure 6. (Colour online) Example 2(b): Our SRM corundum sample turned out to be impure with weak impurity lines being observed, three of which are indicated (vertical black lines) by the mismatch between the calculated (blue) lines and related (red) peaks from the processed histogram. If mostly intense Bragg peaks are used for indexing (in the figure, the peaks marked with vertical red bars and red dots), the correct Al_2O_3 cell is found with very high FOMs: $M(20) = 235.2$ and $F(20) = 137.9(0.0020, 74)$.
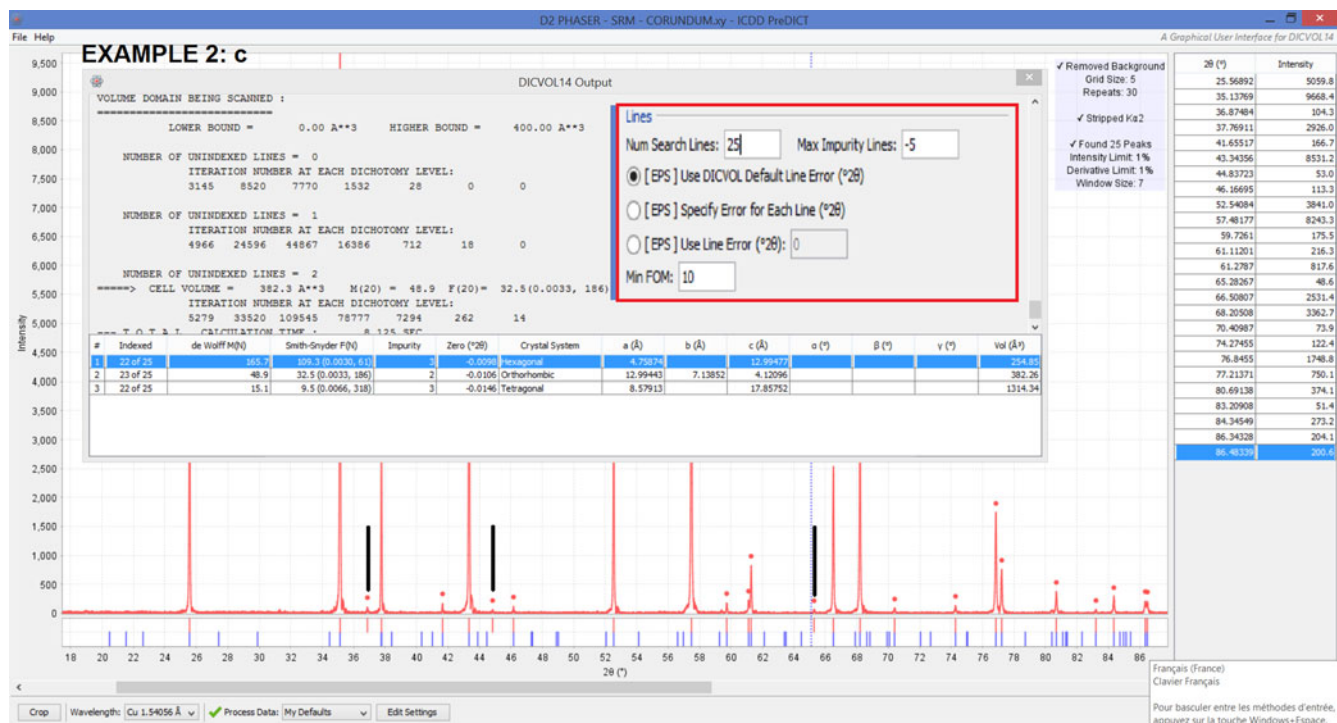
Figure 7. (Colour online) Example 2(c): If the three impurity lines (black vertical bars) are now also included in the starting indexing set consisting of 25 (= 20 + 5) lines (in the figure, vertical red bars and red dots), and up to five impurity peaks are now allowed as part of the indexing calculation, the correct corundum unit cell is again found with very high FOMs: M(20) = 165.7 and F(20) = 109.3(0.0030,61). Requesting up to −5 impurities (see the insert) instead of +5 is a coded way to execute a more exhaustive (but still not fully complete) DICVOL14 search (cf. Dicvol14 manual, v2).
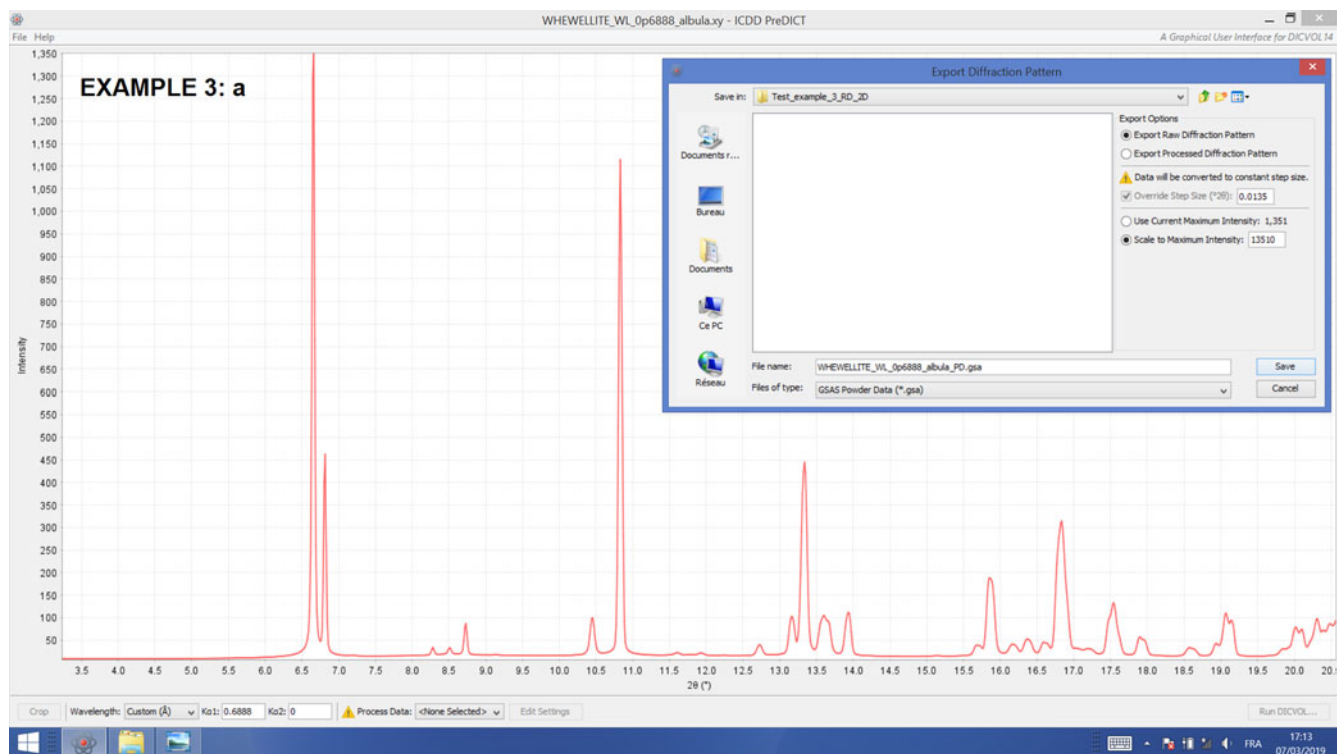

Figure 8. (Colour online) Example 3(a): Monochromatic synchrotron 2D diffraction data ($\lambda = 0.6888$ Å) on a human kidney stone (whewellite) were collected using a 2D DECTRIS EIGER X 9 M detector at the SOLEIL/PROXIMA 2A macromolecular beamline. The data were subsequently converted into a 1D histogram (red line) using the freely available ALBULA software. An ASCII ".XY" dataset is obtained, featuring a decreasing 2θ-step from 0.0143° to 0.0126° across the entire diffractogram, and thereby unsuitable for direct conversion to the ".GSA" format (Larson and Von Dreele, 2004). The PreDICT feature displayed in the inset addresses this situation once a constant 2θ-step has been selected by the user (e.g., the 0.0135° average value). The starting ALBULA 1D histogram can then be suitably interpolated and transformed into a compliant GSAS file now allowing for straightforward subsequent Le Bail/Rietveld refinements.

V. A TYPICAL EXAMPLE INVOLVING A 1D REAL DATASET

Although definitely not the first choice to attempt indexing on a new unknown chemical compound, polychromatic data (e.g., $CuK\alpha_1K\alpha_2$) from a laboratory instrument (e.g., BRUKER/AXS D2PHASER) can in principle be handled by our PreDICT software, once the starting X-ray histogram in binary format [".RAW"] has been converted to ASCII for instance using the freely available PowDLL software (Kourkoumelis, 2013). Subsequent data processing possibly involves (i) background removal, (ii) smoothing, and then mandatorily (iii) $CuK\alpha_2$ or $MoK\alpha_2$ stripping, yielding the (pre)processed diffraction data. Bragg peak selection for subsequent indexing comes in as the next step. One can use the corundum/Al_2O_3 SRM (Standard Reference Material: Bruker AXS Korundprobe A26-B26-S) usually provided with D2 PHASER desktop diffractomers to illustrate the above-mentioned pre-processing phase (Figure 5). Let it be with or without impurities (by ignoring weak peaks), the correct unit cell of the SRM is found straightforwardly (Figures 6 and 7). Once PreDICT has been run and it is observed that there are three impurity diffraction peaks (at $2\theta = 36.88°$, $44.83°$, $65.29°$), the latter values are inserted into the Sieve +/PDF-4+ 2018 database (ICDD, 2019) and software. The impurity phase is found to most likely be magnesium aluminum oxide ($MgAl_2O_4$).

VI. A TYPICAL EXAMPLE INVOLVING A 2D REAL DATASET

Two-dimensional (2D) diffraction at synchrotron macromolecular beamlines is being used increasingly to index, solve, and Rietveld-refine structures from powder data (e.g., Royappa et al., 2018; Horwitz et al., 2019). The preliminary step is to reduce the 2D binary image to a 1D ASCII ".XY" histogram featuring a non-equistepped 2θ increment, for instance by making use of the freely available DECTRIS/ALBULA software. This is not precluding the indexing of powder patterns or to the structure solution using FOX or EXPO, but becomes a problem for the final stage of the data analysis, the Le Bail and Rietveld refinements. The added feature in PreDICT, depicted in Figure 8, circumvents this difficulty.

Two-dimensional-borne powder diffraction patterns are mandatory when too long an exposure to the X-ray beam may prove fatal to the samples, for instance in the case of biological samples (e.g., human kidney stones as in Figures 8 and 9). The much shorter (by a factor of about 25–30) data collection time comes at a price: broader peaks with slightly
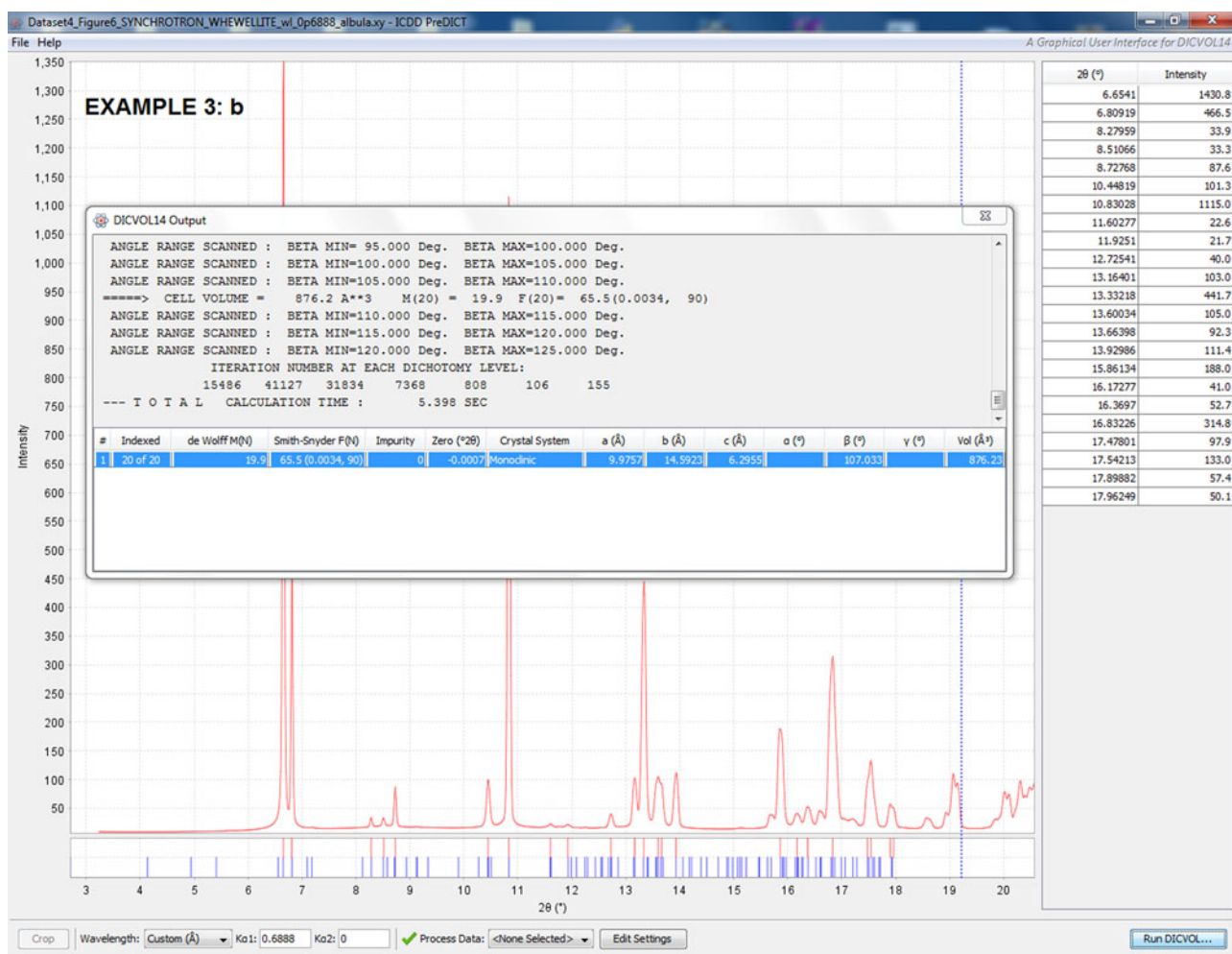

Figure 9. (Colour online) Example 3(b): In spite of the somewhat large non-equistepped 2θ steps (averaged value: 0.0135°), the correct monoclinic unit cell (Tazzoli and Domeneghetti, 1980) is readily found by DICVOL14 with quite an acceptable FOM M(20) = 19.9, albeit in a different setting. The unit cell found by DICVOL14 is rightly flagged as primitive (*P*) in the DICVOL14.ORD output file and the *P*2$_1$/*n* (another setting of *P*2$_1$/*c* space group (#14) accounts for the unobserved indexed reflections. *Note that the original non-equistepped X-ray powder diffraction pattern was used for indexing.*

deformed shapes, increased overlap of the Bragg peaks, and so on. Only the experienced user should venture into indexing in such cases, although quite often most successfully.

The last real data example described in this section and commented in the captions of Figures 8 and 9 emphasizes the fact that the unit cell is not uniquely defined: only the reduced unit cell is (Santoro and Mighell, 1970; Burzlaff et al., 1983). In DICVOL04/14, the reduced cell is used to identify equivalent triclinic and monoclinic solutions (see Boultif and Louër, 2004). In the output files, the reduced cell is reported for a triclinic solution and its conversion to the conventional cell for a monoclinic solution.

VII. CONCLUSION

In this paper, we have presented the main functionalities of our GUI PreDICT for DICVOL14, which stands as the first DICVOL14 GUI to the best of our knowledge. The scope and size of this interface have been strictly limited in order to ensure portability and ease of use. A preliminary version was tested during Crystallographic Intensive Courses and Clinics in the USA, respectively, sponsored by the ACA (American Crystallographic Association) and the ICDD (International Centre for Diffraction Data). As has been abundantly mentioned in the past, the indexing of Powder Diffraction patterns requires user intervention and the best possible software will only provide the user with possible solutions rather than full certainty of correct indexing until a chemically plausible crystal structure is solved and refined. The use of complementary indexing methods can only help the user sort out and validate a possible solution (Bergmann et al., 2004). Our recommended next best choice for indexing software is another freely available package, N-TREOR, as implemented in the EXPO software suite (Altomare et al., 2000). When both DICVOL14/PreDICT and N-TREOR/EXPO point to the same unit cell and possibly lattice centering, the future looks bright.

SUPPLEMENTARY MATERIAL

The supplementary material for this article, which includes all the one dimensional diffractograms (simulated and raw data) discussed in this paper, can be found at https://doi.org/10.1017/S0885715619000514. The complete software package itself (PreDICT + DICVOL14) can be freely dowloaded as a unique ZIP file from the ICDD website, www.icdd.com/index.php/predict/.

ACKNOWLEDGMENTS

ALBULA Software. (**2015**). Version 3.2.0, published by DECTRIS Ltd. https://www.dectris.com/products/albula-software.

Altomare, A., Giacovazzo, C., Guagliardi, A., Moliterni, A., Rizzi, R., and Werner, P.-E. (**2000**). "New techniques for indexing: N-TREOR in EXPO," J. Appl. Crystallogr. **33**, 1180–1186.

Altomare, A., Cuocci, C., Giacovazzo, C., Moliterni, A., Rizzi, R., Corriero, N., and Falcicchio, A. (**2013**). "EXPO2013: a kit of tools for phasing crystal structures from powder data", J. Appl. Crystallogr. **46**, 1231–1235.

Bergmann, J., Le Bail, A., Shirley, R., and Zlokazov, V. (**2004**). "Renewed interest in powder diffraction indexing," Z. Kristallogr. **219**, 783–790.

Boultif, A. and Louër, D. (**1991**). "Indexing of powder diffraction patterns for low-symmetry lattices by the successive dichotomy method," J. Appl. Crystallogr. **24**, 987–993.

Boultif, A. and Louër, D. (**2004**). "Powder pattern indexing with the dichotomy method," J. Appl. Crystallogr. **37**, 724–731.

Burzlaff, H., Zimmerman, H., and de Wolff, P. M. (**1983**). "9. Crystal lattices," in *International Tables for Crystallography*, edited by T. Hahn (D. Reidel Publ. Co, Dordrecht), vol. A, pp. 733–744.

Coelho, A. A. (**2017**). "An indexing algorithm independent of peak position extraction for X-ray powder diffraction patterns," J. Appl. Crystallogr. **50**, 1323–1330.

David, W. I. F., Shankland, K., van de Streek, J., Pidcock, E., Motherwell, W. D. S., and Cole, J. C. (**2006**). "DASH: a program for crystal structure determination from powder diffraction data." J. Appl. Crystallogr. **39**, 910–915.

De Wolff, P. M. (**1968**). "A simplified criterion for the reliability of a powder pattern indexing," J. Appl. Crystallogr. **1**, 108–113.

Favre-Nicolin, V. and Černý, R. (**2002**). "FOX, free objects for crystallography: a modular approach to ab initio structure determination from powder diffraction," J. Appl. Crystallogr. **35**, 734–743.

Fawcett, T. G., Kabekkodu, S. N., Blanton, J. R., and Blanton, T. N. (**2017**). "Chemical analysis by diffraction: The Powder Diffraction File™," Powder Diffr. **32**, 63–71.

Horwitz, N. E., Xie, J., Filatov, A. S., Papoular, R. J., Shepard, W. E., Zee, D. Z., Grahn, M. P., Gilder, C., and Anderson, J. S. (**2019**). "Redox-active 1D coordination polymers of iron-sulfur clusters," J. Am. Chem. Soc. **141**, 3940–3951.

ICDD (**2019**). PDF-4+ 2019 (Database), edited by Dr. Soorya Kabekkodu (International Centre for Diffraction Data, Newtown Square, PA, USA).

Kourkoumelis, N. (**2013**). "PowDLL, a reusable .NET component for interconverting powder diffraction data: recent developments," ICDD Annual Spring Meetings, (ed. Lisa O'Neill), Powder Diffr. **28**, 137–148.

Langford, J. I. and Louër, D. (**1996**). "Powder diffraction," Rep. Prog. Phys. **59**, 131–234.

Larson, A. C. and Von Dreele, R. B. (**2004**). General Structure Analysis System (GSAS) (Report No. LAUR 86-748), Los Alamos National Laboratory, Los Alamos, NM.

Le Bail, A. (**2005**). "Whole pattern decomposition methods and applications: a retrospection," Powder Diffr. **20**, 316–326.

Louër, D. (**1992**). "Automatic indexing: procedure and applications," Natl. Inst. Standards Technol. Special Publication **846**, 92–104.

Louër, D. and Louër, M. (**1972**). "Méthode d' Essais et Erreurs pour l'indexation automatique des diagrammes de Poudre," J. Appl. Crystallogr. **5**, 271–275.

Louër, D. and Boultif, A. (**2014**). "Some further considerations in powder diffraction pattern indexing with the dichotomy method," Powder Diffr. **29**(S2), S7–S12.

Macrae, C. F., Bruno, I. J., Chisholm, J. A., Edington, P. R., McCabe, P., Pidcock, E., Rodriguez-Monge, L., Taylor, R., van de Streek, J., and Wood, P. A. (**2008**). "Mercury CSD 2.0 – new features for the visualization and investigation of crystal structures," J. Appl. Crystallogr. **41**, 466–470.

Putz, H. and Brandenburg, K. (**2018**). "MATCH! Phase Identification from Powder Diffraction," CRYSTAL IMPACT. https://www.crystalimpact.de/match.

Rachinger, W. A. (**1948**). "A correction for the $\alpha_1 \alpha_2$ doublet in the measurement of widths of X-ray diffraction lines," J. Sci. Instrum. **25**, 254–255.

Rietveld, H. M. (**1969**). "A profile refinement method for nuclear and magnetic structures," J. Appl. Crystallogr. **2**, 65–71.

Roisnel, T. and Rodriguez-Carvajal, J. (**2001**). "WinPLOTR: a windows tool for powder diffraction pattern analysis," Mater. Sci. Forum. **378–381**, 118–123.

Royappa, A. T., Tran, C. M., Papoular, R. J., Khan, M., Marbella, L. E., Millstone, J. E., Gembicky, M., Chen, B., Shepard, W., and Elkaïm, E.

(**2018**). "Copper(I) and Gold(I) thiolate precursors to bimetallic nanoparticles," Polyhedron. **155**, 359–365.

Santoro, A and Mighell, A. D. (**1970**). "Determination of reduced cells," Acta Crystallogr. **A26**, 124–127.

Savitzky, A. and Golay, M. J. E. (**1964**). "Smoothing and differentiation of data by simplified least squares procedures," Anal. Chem. **36**, 1627–1639.

Shirley, R. (**1980**). "Data accuracy for powder indexing," Natl. Bureau Standards Special Publication **567**, 361–382.

Smith, G. S. and Snyder, R. L. (**1979**). "F_N: a criterion for rating powder diffraction patterns and evaluating the reliability of powder-pattern indexing," J. Appl. Crystallogr. **12**, 60–65.

Sonnefeld, E. J. and Visser, J. W. (**1975**). "Automatic collection of powder data from photographs," J. Appl. Crystallogr. **8**, 1–7.

Tazzoli, V. and Domeneghetti, C. (**1980**). "The crystal structures of whewellite and weddellite: re-examination and comparison," Am. Mineral. **65**, 327–334.